Report on the mineralogical and geochemical characterisation of Hawai'i ash for the assessment of respiratory health hazard

Claire J Horwell[1]
Sabina Michnowicz[1]
Jennifer Le Blond[2]

[1]Institute for Hazard and Risk Research, Department of Earth Sciences, Durham University, Science Labs, Durham DH1 3LE, UK.
[2]Department of Geography, University of Cambridge, Downing Place, Cambridge CB2 3EN, UK.

Contents

Executive Summary

The mineralogical and geochemical characteristics of a suite of volcanic ash samples from Kilauea volcano, Hawai'i were determined in order to assess the potential respiratory health hazard.. Key results are as follows:

- **Bulk composition** analysis (XRF) of the samples showed that the samples are basaltic – basaltic andesite (46.7-56.3 wt. % SiO_2).

- **Grain size** analysis found the samples to be very variable. The quantity of respirable (< 4 μm) particles ranged from 0.0-6.8 vol. %.

- **Morphology** – the ash particles are glassy and angular with occasional blocky and fibrous particles. The blocky particles are anhydrite, whereas the fibrous ones are gypsum. Gypsum is not considered to be a health hazard because of its solubility in the lung.

- **Surface area** – the surface area of two samples was very low (0.1 and 0.8 m^2g^{-1}) which is in keeping with analyses from other basaltic volcanoes. A third sample (Hawa_09) was re-tested with krypton, following difficulties with nitrogen absorption, giving a result of 3.9 m^2g^{-1}. This is not comparable, however, with the nitrogen readings given above.

- **Surface reactivity** – all samples generated hydroxyl radicals (through an iron-catalysed reaction which can potentially be a carcinogenic and inflammatory factor in the lungs). Two samples generated 0.1 and 0.6 μmol m^{-2} hydroxyl radicals after 30 mins. of reaction which is at the lower end of the range of results obtained previously for other volcanic ash samples. One sample however (Hawa_04), generated a high number of hydroxyl radicals (7.0 μmol m^{-2}) after 30 mins.

- **Iron release** – Two of the samples released relatively low amounts of total iron (a measure of the iron available for surface reactions) (23.0 and 86.9 μmol m^{-2} after 7 days incubation). One sample (Hawa_04) released substantial quantities of iron (728.2 μmol m^{-2} after 7 days incubation) and this correlated well with the high number of radicals generated by this sample.

Health message

The finer samples of Kilauea ash are sufficiently fine-grained to have the potential to trigger asthma attacks in susceptible people, and aggravate respiratory symptoms in people with chronic lung problems, if exposure is substantial. All people should wear masks in situations where exposure to the ash is going to be high, e.g., dry, windy days and where heavy traffic or tasks such as ash removal create dust in the air.

In public health terms, the potential for the development of long-term respiratory problems depends mainly upon the amount of crystalline silica in the ash and proportion of the ash which can be easily breathed into the deep parts of the lung. Taking the results of this study, and the experience acquired from other volcanoes over the last 25 years, the health hazard is low unless frequent eruptive activity commences which repeatedly exposes the population to high ash levels over long durations. In this case, careful monitoring of exposure and ash composition is required to make a full risk assessment.

1. Introduction

1.1 Aims

To carry out a mineralogical and geochemical analysis of the ash erupted from Halema`uma`u Crater, Kilauea Volcano, Hawai'i (March-April 2008) to assess the potential for the ash to pose a respiratory health hazard.

1.2 Ash analysis protocol

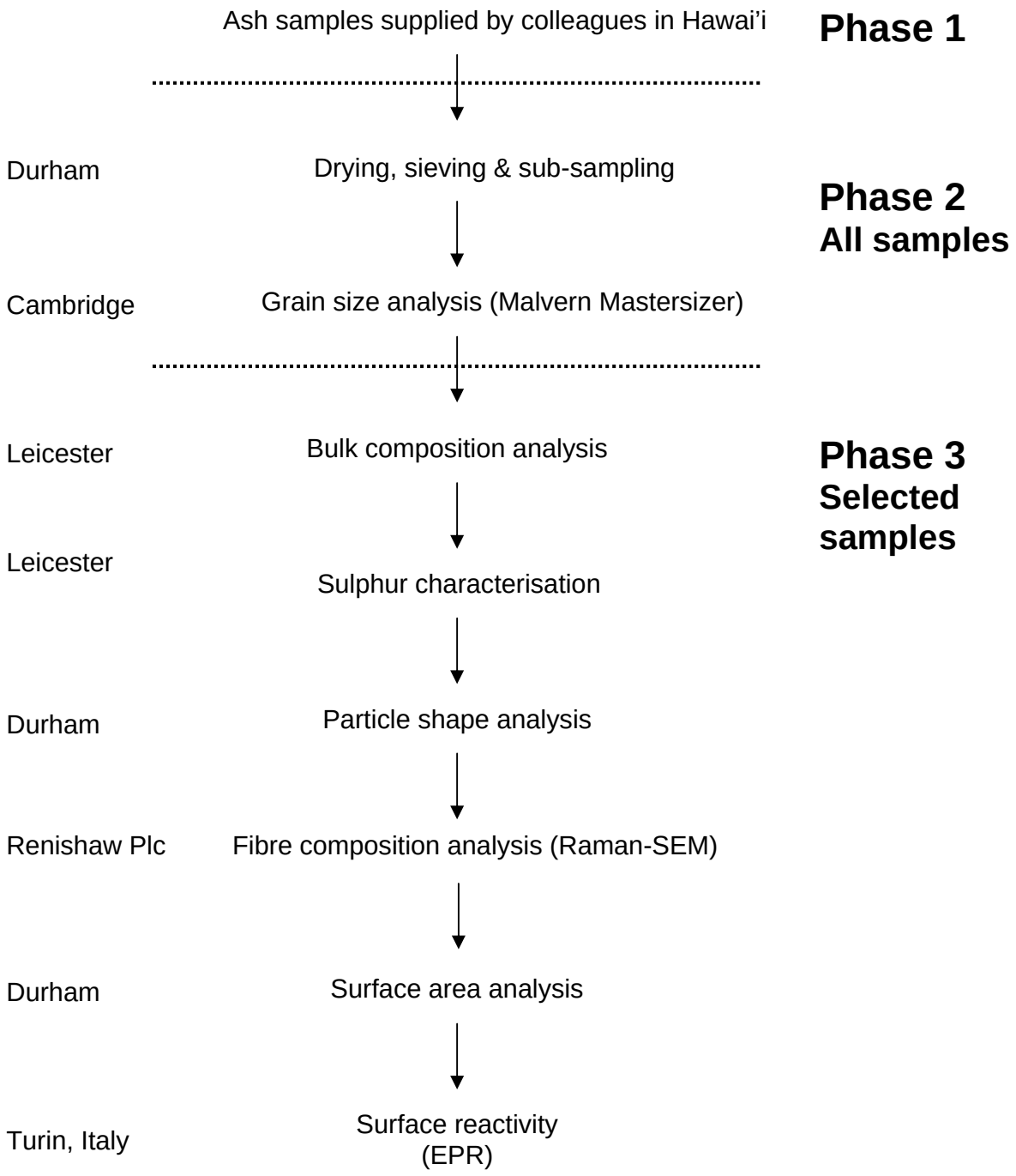

1.3 Samples

Table 1.3.1 shows the location and details of collection of the Hawai'i ash samples. Figure 1.3.1 shows the location of the individual samples in relation to Kilauea volcano. Samples were sent to Durham University from the Hawaiian Volcano Observatory. They were collected within 24 hours of deposition. Information about the samples is as follows:

Table 1.3.1 Information for the samples analysed in this report

Sample No.	HVO number	Collection Date	Latitude	Longitude	Contamination /rain
Hawa_01	KS08-40T	20/03/08	19.401956	-155.28126	No
Hawa_02	KS08-03T	25/03/08	19.402986	-155.28122	No
Hawa_03	KS08-10T	27/03/08	19.402986	-155.28122	No
Hawa_04	Sandhill	27/03/08	19.395000	-155.29370	No
Hawa_05	A7-0641-4/2/08	02/04/08	19.403932	-155.28019	No
Hawa_06	A8-1321-4/3/08	03/04/08	19.404237	-155.27984	No
Hawa_07	A5-0637-4/10/08	10/04/08	19.403065	-155.28036	No
Hawa_08	A7-0700-4/16/08	16/04/08	19.403932	-155.28019	No
Hawa_09	A7-0732-4/17/08	17/04/08	19.403932	-155.28019	No

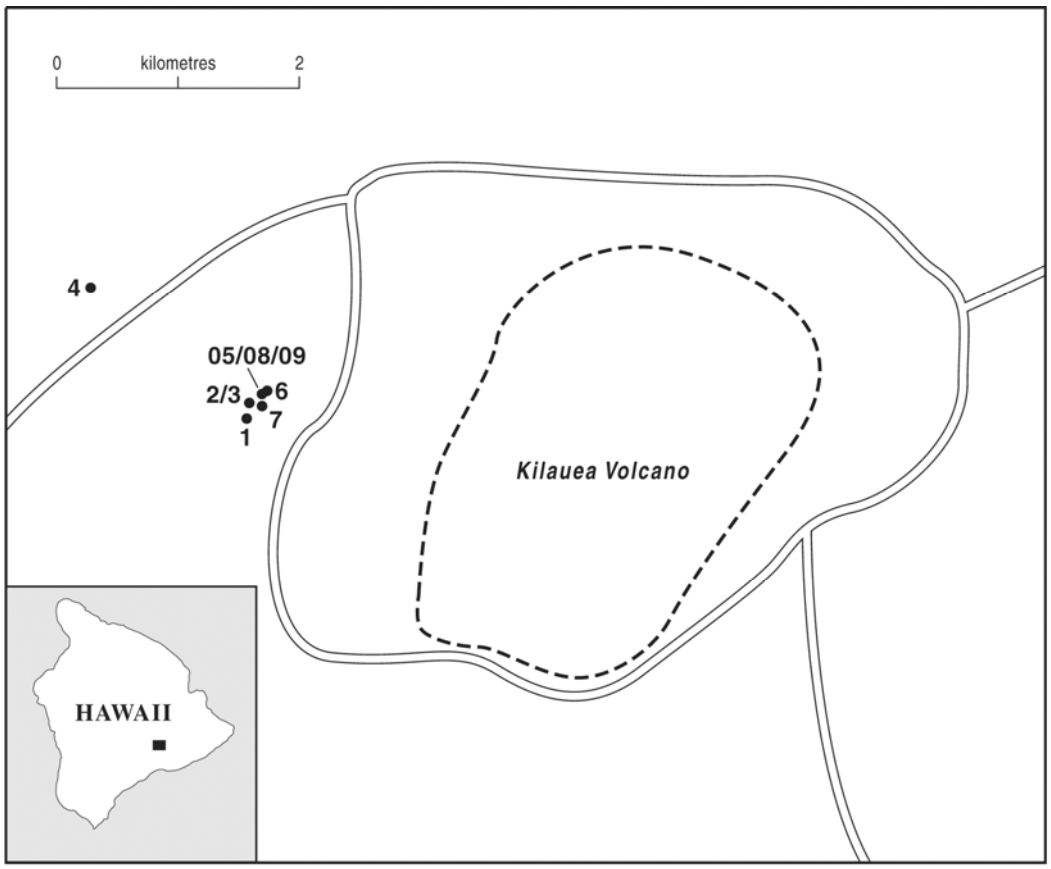

Figure 1.3.1 Location of collection of samples analysed for this report

1.4 Geological setting

Kilauea volcano overlaps the east flank of Mauna Loa volcano and has been Hawai'i's most active volcano during historical times. It was formed in several stages about 1500 years ago and during the 18th century. Eruptions have also originated from the East and SW rift zones, which extend to the sea on both sides of the volcano. About 90% of the surface of the basaltic shield volcano is formed of lava flows less than about 1100 years old; 70% of the volcano's surface is younger than 600 years. A long-term eruption from the East rift zone that began in 1983 (known as the Pu`u `O`o eruption) has produced lava flows covering more than 100 sq km which have added land to the coastline. Kilauea shares the Hawaiian hot spot with its larger active sibling Mauna Loa and with Loihi seamount.

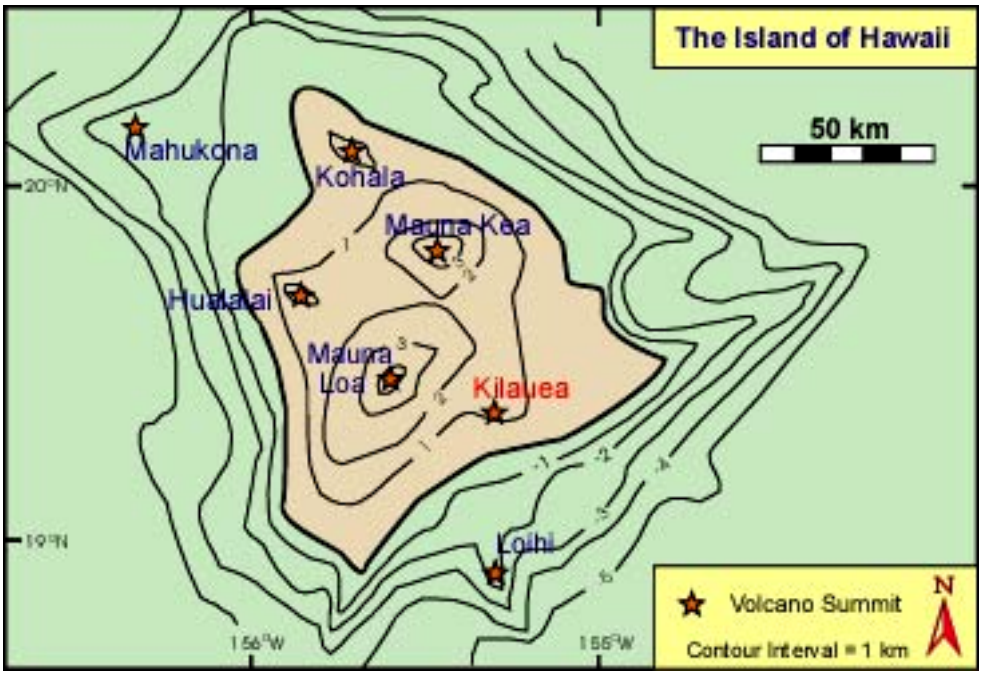

Figure 1.4.1 Map of Big Island, Hawai'i
(from: http://www.soest.hawaii.edu/GG/HCV/kil-general.html)

1.5 2008 eruption timeline

June 2007 – March 2008 Precursor activity and eruption start

A number of significant changes on Kīlauea volcano have taken place in 2008, both at its summit and along its east rift. In March, summit sulfur dioxide (SO_2) emissions reached record high levels; a new vent opened in Halema`uma`u Crater; a small explosive eruption occured at Kīlauea's summit, the first since 1924; and lava flowed into the sea for the first time in over eight months. Events leading up to these changes date back to at least mid-2007, when an intrusion on June 17 disrupted the supply of magma to Pu`u `Ō `ō, the long-lived vent on Kīlauea's east rift. On the 24 March a continuous emission of lithic-rich ash began from the new vent opening in Halema`uma`u Crater. The plume, a dusty-brown colour, is shown in Figure 1.5.1. The top of the ash plume reached 0.5 - 1.0 mile above ground level, requiring Hawai`i aviation agencies to be notified of the potential hazard to aircraft.

Figure 1.5.1 Ash emitting from Halema`uma`u Crater in March
(photograph from: http://hvo.wr.usgs.gov/kilauea/update/archive/2008/Mar/20080324-6790-CCH_L.jpg)

April 2008 – Explosive activity

A second explosion from the new vent in Halema`uma`u Crater occurred on 9 April 2008; the explosion was smaller in magnitude than the one on 19 March 2008, but enlarged the vent by 5-10 metres. The explosion ejected considerably less rocky material than the 19 March event. Hawai`i County Civil Defense received reports of ash fall in Pahala (~ 19 miles from summit). A further explosion occurred on 16 April depositing a thin layer of pink-coloured lithic ash as seen in Figure 1.5.2.

Figure 1.5.2 A USGS vehicle travelling on Crater Rim Drive near Halema`uma`u Crater creates tracks in the thin layer of pink ash ejected in the April 16 explosion.

May - July 2008 – Emissions of SO_2 and ash, and magma movement
Very small amounts of ash were emitted during this period. There were elevated emissions of SO_2 at Halema`uma`u Crater and even higher quantities emitted from Pu`u `Ō`ō. One of the most unusual aspects of the current eruption was that there had been no change in surface deformation trends; however, on 24 June tiltmetres began to show inflation for the first time since 21 July 2007. The intensity of the glow at the summit vent correlated with bursts of seismic tremor indicating that gas bubbles were bursting through a crusted lava surface beneath the Halema`uma`u vent and the lava surface was rising. Lava broke out of the tube system, both on the east rift zone and above the Royal Gardens subdivision. At the same time, littoral explosions at the ocean entry occurred during early July. All of these signs point to a lava tube system that was full to the point of overflowing. Taken together, this evidence suggests that Kīlauea was engorged with magma, starting in late June. Increased magma in the caldera and east rift areas resulted in inflation of the summit and Pu`u `Ō`ō and, possibly, rising of the lava column in the Hamema`uma`u vent. Magma was also being delivered to the eruption site at a greater rate than normal, resulting in numerous surface lava flows.

August 2008 – Explosive activity and lava flows
There was a fourth explosive eruption at Halema`uma`u on 1 August which scattered rocky debris along a narrow band downwind of the crater vent; the summit plume occasionally turned brown as ash was erupted from the vent. In response to a summit deflation-inflation event, lava stopped flowing through tube system and into ocean, four days later however, lava made its way back down the tube and flowed into the ocean at the Waikupanaha entry.

Sources for Sections 1.4 & 1.5:
- SI/USGS Weekly Volcanic Activity Reports (sent to Volcano Listserv mailing list)
- http://hvo.wr.usgs.gov/kilauea/timeline/
- http://160.111.247.173/world/volcano.cfm?vnum=1302-01-
- http://www.soest.hawaii.edu/GG/HCV/kil-general.html

2. Analytical Methods

2.1 Sample analysis summary

Table 2.1.1 gives a summary of the analyses carried out on each sample.

Table 2.1.1 Analysis summary

Sample	Malvern	XRF	SEM	BET	EPR	Iron
Hawa_01	√	√	√	√	√	√
Hawa_02	√					
Hawa_03	√		√			
Hawa_04	√	√		√	√	√
Hawa_05	√					
Hawa_06	√					
Hawa_07	√					
Hawa_08	√					
Hawa_09	√	√	√	√	√	√

2.1.1 Sample preparation

All samples were dried in an oven set at 80°C for at least 12 hours. Samples were then sieved (Endecott stainless steel sieves) through both a 2mm and 1mm sieve in order to remove a) particles greater than 2mm diameter, which are considered larger than the volcanic ash fraction; b) particles close to 2mm which may potentially damage the Malvern Mastersizer. The samples were weighed prior to drying, following drying, and from each sieve fraction (see Table 2.1.2). All analyses in this report were carried out on the < 1mm except where stated.

Table 2.1.2 Weight (g) of ash fractions following sieving.

Sample	<1 mm	1-2 mm	> 2 mm
Hawa_01	22.18	27.42	49.29
Hawa_02	108.22	0.13	0
Hawa_03	84.34	0.14	0.01
Hawa_04	18.03	0	0
Hawa_05	8.68	0.04	0
Hawa_06	3.21	6.15	0.98
Hawa_07	9.64	7.81	4.47
Hawa_08	3.53	1.35	0.42
Hawa_09	32.7	12.57	7.39

2.2 Bulk composition – X-ray fluorescence

When a sample is bombarded with high energy X-rays, the sample is ionised (i.e. an electron/several electrons are ejected from the atom) and becomes inherently unstable. Energy, in the form of a photon, is released as the atom strives to become stable once more. The energy released is characteristic of the atoms present. XRF is, therefore, used to determine the bulk oxide elemental composition of a sample. In turn, the bulk compositions are used to classify the type of magma erupted.

2.2.1 Method

Samples were analysed on the PANalytical Axios Advanced XRF spectrometer at the Department of Geology, University of Leicester. Major elements were determined on fused glass beads prepared from ignited powders, with a sample to flux ratio 1:10, 100% Li tetraborate flux.

2.2.2 Results

The results are quoted as a component oxide weight percent, re-calculated to include loss on ignition (LOI) (Table 2.2.1, below). Figure 2.2.1 plots the results on a total alkali-silica plot (TAS plot) in order to define the magmatic composition of the samples.

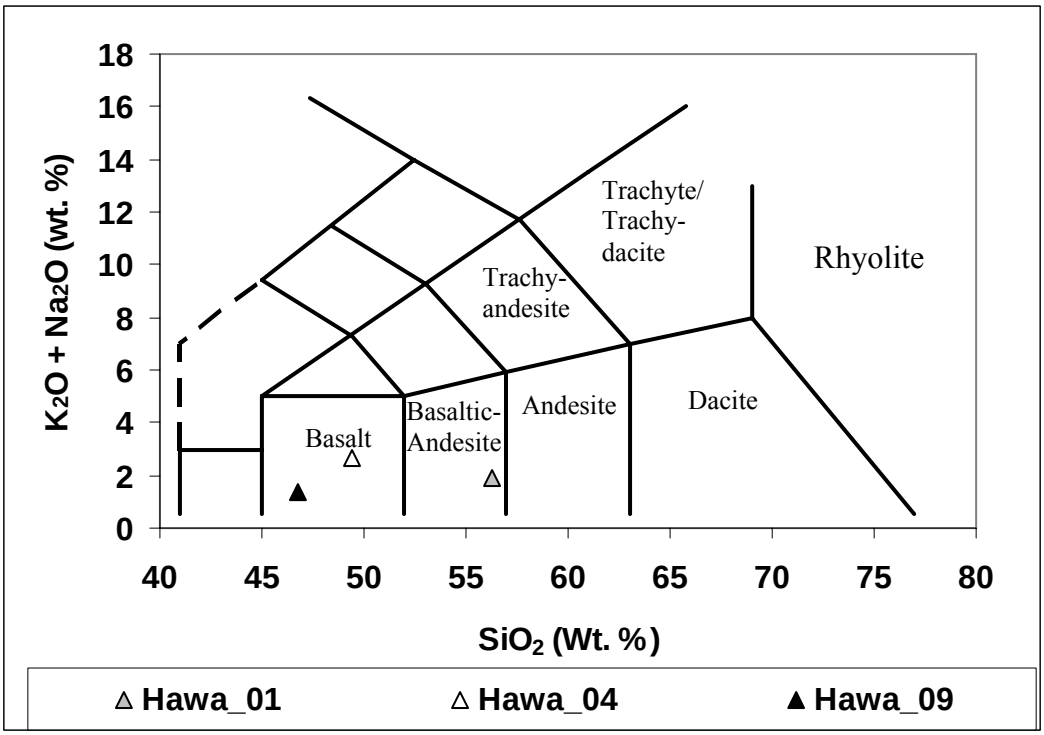

Figure 2.2.1. Results from the XRF analysis of the volcanic ash samples, plotted on a TAS (total alkali versus silica content[1]) plot.

Using the IUGS (International Union of Geological Sciences) classification of igneous rocks based on the alkaline content (see Fig. 2.2.1), the samples are basaltic/basaltic andesite. However, these results are distorted by the fact that both samples Hawa_01 and Hawa_09 are

skewed because they contain significant quantities of sulphur (7.2 & 17.4 wt. % SO_3 respectively (Table 2.2.1).

To determine the cause of the sulphur, X-ray diffraction (XRD) was carried out at the University of Leicester to identify the crystalline components in a bulk powdered sample. The peak labelled 1 in Figure 2.2.2 below is anhydrite ($CaSO_4$).

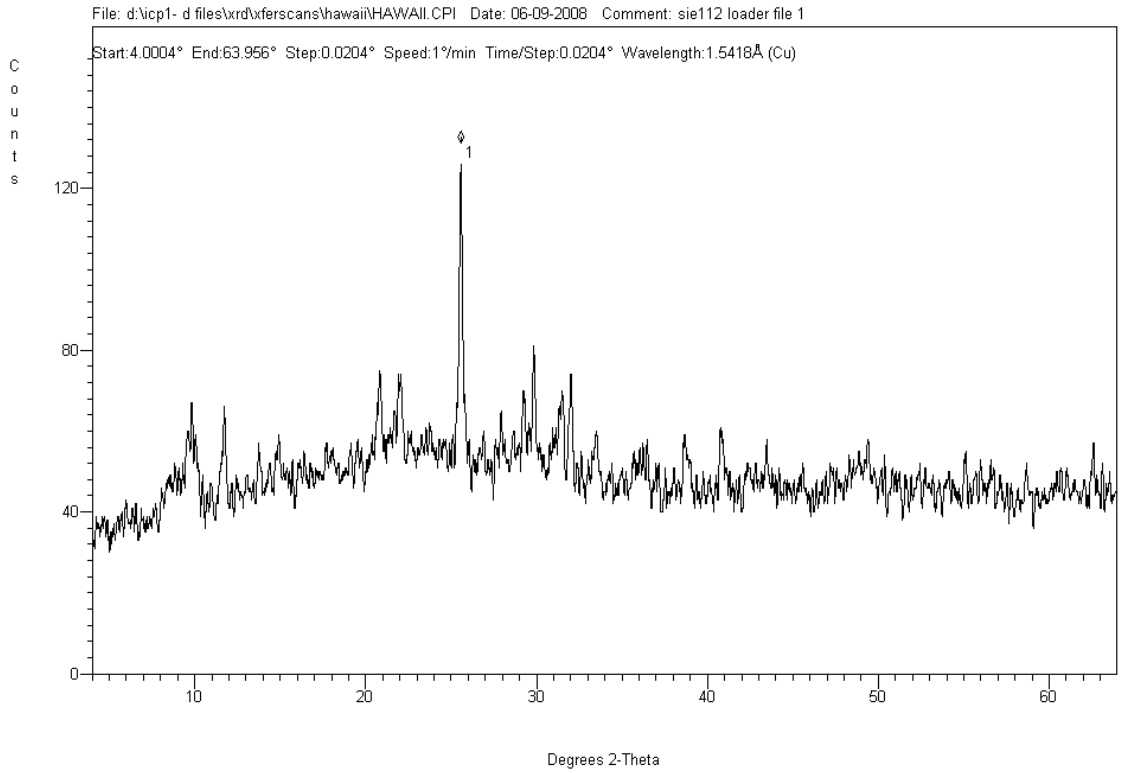

Figure 2.2.2 XRD pattern for the Hawa_09 ash sample.

Table 2.2.1. Results of the XRF analysis for the volcanic ash samples (wt. %)

Sample	SiO_2	TiO_2	Al_2O_3	Fe_2O_3	MnO	MgO	CaO	Na_2O	K_2O	P_2O_5	SO_3	LOI	Total
Hawa_01	56.30	2.69	7.13	7.15	0.085	3.64	10.37	1.36	0.540	0.150	7.24	3.19	99.85
Hawa_04	49.39	2.83	12.18	13.31	0.180	8.39	11.13	2.17	0.514	0.239	0.12	0.11	100.35
Hawa_09	46.73	2.27	4.71	4.56	0.047	2.25	14.09	1.01	0.365	0.126	17.37	7.21	100.73

2.3 Grain size analysis – Malvern Mastersizer

The Malvern Mastersizer 2000 is a laser diffraction particle size analyser, which measures the total number of particles within the 0.2-2000 μm range. The results are from the Malvern Mastersizer 2000 with Hydro MU attachment at the Department of Geography at the University of Cambridge.

2.3.1 Method

The < 1mm fraction was analysed on a Malvern Mastersizer 2000 with Hydro MU attachment at the Department of Geography, Cambridge University, UK. Ultrasonics were used to disaggregate samples and the results below are from an average of three runs. Samples were measured with a refractive index of 1.55 and an absorption coefficient of 0.1 (after Horwell, 2007[2]). The weight data from any sieved particles in the 1-2mm size range (still within the accepted 'ash fraction' of particles < 2mm diameter) were then re-incorporated into the Malvern grain size distributions (see Table 2.1.2).

2.3.2 Results

Table 2.3.1 gives information on the potential effects of each grain size fraction. Results in Table 2.3.2 are the cumulative volume % of grain size within the health-pertinent fractions.

Table 2.3.1. Potential health effects of ash fractions.

Size	Potential Health Effect
< 4 μm	'Respirable' fraction – can enter the alveoli where chronic disease could occur with long-term exposure
< 10 μm	'Thoracic' fraction – can enter past the bronchus, where bronchitis, asthma and other acute diseases may be triggered in susceptible people.
< 15 μm	Can enter the throat, causing rhinitis, laryngitis and irritation

Table 2.3.2 Grain-size results in cumulative volume %

Size (μm)	Hawa_01	Hawa_02	Hawa_03	Hawa_04	Hawa_05	Hawa_06	Hawa_07	Hawa_08	Hawa_09
< 4	2.83	0.42	0.69	2.72	0.98	0.02	4.10	1.99	6.81
< 10	5.05	1.18	1.74	6.59	2.08	0.18	7.23	3.53	13.91
< 15	6.21	1.47	2.18	9.97	2.67	0.28	8.52	4.43	18.72

Table 2.3.2. shows that the grain size distributions vary significantly among samples. The samples, themselves, varied substantially in morphology, with some samples being extremely poorly sorted, whilst others were fairly homogeneous. Some samples contained fragments of Pele's hair (Hawa_03, _05 and_06). Laser diffraction analyzers assume spherical particles so results may be slightly skewed for these samples. Representative sampling is also challenging

for poorly-sorted samples. However all analyses showed consistent results for the three runs with the exception of Hawa_07 which was repeatedly analysed until a reliable result was obtained.

Table 2.3.2 shows that most of the samples contained some respirable (< 4μm) material. The most significant sample, in terms of health hazard, is sample Hawa_09 which contained substantial quantities of < 4 μm particles (6.81 %). This sample was a fine, homogeneous sample of pink/beige ash, with aggregated particles which disaggregated easily with sieving.

Table 2.3.3 shows results published from other volcanoes. It can be seen that the more poorly-sorted Hawaiian ash samples have similar characteristics to other basaltic, low-VEI eruptions, such as Pacaya and Fuego. At least 4 samples (Hawa_01, _04, _07 and _08) are finer, with results having similarities to more explosive eruptions such as seen at Etna or more silicic volcanoes. Sample Hawai_09 is akin to the Vulcanian explosive eruptions observed at the Soufrière Hills volcano and Langila (PNG). Please refer to Horwell 2007 for further information on those eruptions.

Following grain-size analysis, three fine-grained samples (Hawa 01, 04 & 09) were chosen for further mineralogical/geochemical analyses. Hawa_07 was not chosen due to the problems of representative sampling for the grain-size analyses.

Table 2.3.3 Grain size analyses from other volcanoes (from Horwell, 2007[2])

Volcano	Magma type/ Eruption style	VEI*	Grain- size distribution, Cumulative volume %					
			< 1 µm	< 2.5 µm	< 4 µm	< 10 µm	< 15 µm	< 63 µm
Pacaya, Guatemala 1994	Basaltic Stromb.-Vulc.	1	0.00	0.00	0.04	0.41	0.70	2.23
Pacaya, Guatemala 1992	Basaltic Stromb,-Vulc.	1	0.00	0.26	0.76	2.43	3.76	16.60
Fuego, Guatemala 1999	Basaltic Vulcanian	2	0.00	0.00	0.00	0.00	0.00	1.56
Ulawun, Papua New Guinea	Basaltic Strombolian	2	0.00	0.02	0.27	0.88	1.63	4.14
Cerro Negro, Nicaragua	Basaltic Stromb.-Vulc.	2	0.00	0.22	0.64	2.55	4.17	14.64
Tungurahua, Ecuador	Andesitic Stromb.-Vulc.	2	0.65	2.49	4.11	10.49	15.46	41.80
Langila, Papua New Guinea	Bas.-And. Vulcanian	2	0.87	3.29	5.63	13.95	19.83	52.71
Merapi, Indonesia	Bas.-And. Dome collapse	2	1.95	8.02	12.66	27.24	38.11	83.06
Vesuvius, Italy AD79-472	Tephr.-Phon. Stromb.-Vulc.	2-3	0.72	2.09	3.24	7.13	10.14	33.99
Sakurajima, Japan	Andesitic Vulcanian	3	0.00	0.50	0.86	1.95	2.87	14.74
Etna, Italy	Basaltic Strombolian	3	0.27	1.09	1.83	4.59	6.75	22.17
Ruapehu, New Zealand	Andesitic Sub-plinian	3	0.51	2.44	4.14	9.43	13.37	32.19
Soufrière Hills, Montserrat 1997	Andesitic Vulc. explosion	3	1.00	3.60	5.90	13.40	18.50	44.08
Soufrière Hills, Montserrat 1999	Andesitic Dome collapse	3	1.94	6.74	10.70	23.10	31.90	76.88
Soufrière Hills, Montserrat 2003	Andesitic Dome collapse	3	2.70	7.87	11.47	22.49	30.75	74.63
Fuego, Guatemala 1974	Basaltic Subplinian	4	0.88	2.43	3.66	7.99	12.04	46.64
El Reventador, Ecuador	Andesitic Vulcanian	4	0.90	3.21	4.88	10.16	15.12	72.93
Mt St Helens, USA	Dacitic Plinian	5	1.69	7.39	11.74	24.50	33.15	78.76
Vesuvius, Italy AD79	Tephr.-Phon. Plinian	5	4.81	11.62	16.93	32.83	43.39	83.70
Pinatubo, Philippines 3/6/91	Dacitic Plinian	6	1.07	5.49	8.97	17.88	23.12	54.05
Pinatubo, Philippines 4/7/91	Dacitic Sub-plinian	6	1.33	6.18	9.82	18.93	24.34	60.69

Amount of material for health-pertinent fractions found in selected samples of volcanic ash. The table is ordered by increasing VEI (volcanic explosivity index). Grain-size distributions measured on Malvern Mastersizer 2000 with Hydro MU.

2.4 Particle Morphology and Composition – SEM and Raman

2.4.1 Particle morphology

Scanning electron microscopy allows the user to observe the morphology of volcanic ash. We used SEM to determine the dimensions of Pele's hair fragments from sample Hawa_03 to ensure that they are not respirable or fibrous* and to carry out a general inspection of the samples to check for any unusual features. Analysis was carried out on uncoated samples in a Hitachi TM-1000 Tabletop SEM Microscope in the Department of Earth Sciences, Durham University.

2.4.1.1 Methods

Stubs were assembled by sticking a carbon sticky pad on to an aluminium SEM stub. A small (0.5 mm diameter) polycarbonate disc was then stuck to the sticky pad and ash was either sprinkled or smeared (with ethanol) onto the disc. Samples were left un-coated due to instrumental problems.

2.4.1.2 Results

The fragments of Pele's hair that were examined were approximately 2mm long and 40 μm wide, decreasing to 10 μm diameter at the tips. No respirable hairs were found although it is possible that fragmentation of a hair could result in respirable particles being created from the tips of the hairs. The hairs would have to form a substantial proportion of a sample for this to pose a significant health hazard.

Although the Pele's hair was not fibrous, we did identify occasional fibrous crystals in the samples (e.g. in Hawa_09, Figure 2.4.1).

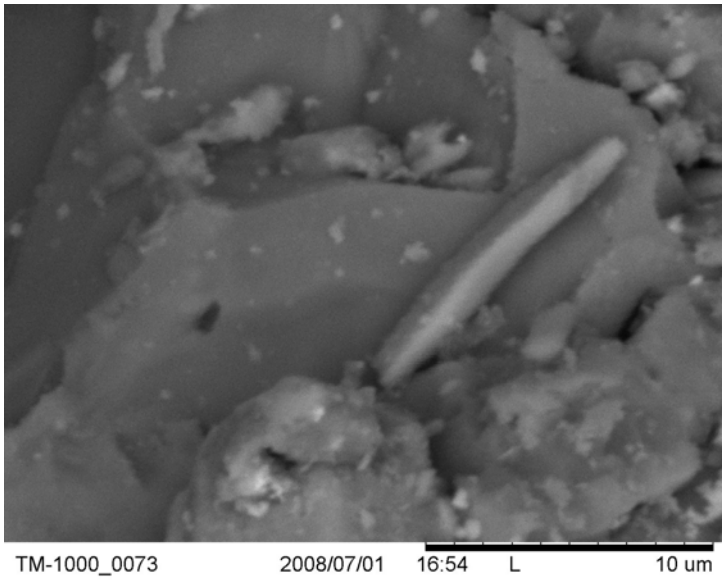

Figure 2.4.1 A fibrous crystal observed in sample Hawa_09 by SEM.

* Only fibres over 5 μm in length with an aspect ratio of ≥ 3:1 and a diameter of less than 3 μm. WHO. 1986. Asbestos and other natural mineral fibres. Environmental Health Criteria 53. Geneva, World Health Organisation.

2.4.2 Particle composition

Scanning electron microscopy also allows the user to study the composition of individual ash particles at high magnification. Here we used SEM to determine the exact composition of the fibrous crystals observed (Section 2.4.1). The analysis was carried out using the state-of-the-art SEM-Raman facility at Renishaw Plc, Gloucestershire.

SEM with energy dispersive spectroscopy (SEM-EDS) allows the user to identify the *elemental* composition of a particle. SEM-Raman allows accurate identification of the *mineralogical* composition of an individual particle. Raman spectroscopy relies on the inelastic scattering which occurs when the sample is subjected to a laser beam. The laser interacts with phonons in the sample, which causes the laser photons to shift up or down in energy. This energy shift is characteristic to, and can yield, information about the sample. The Raman spectroscopy system at Renishaw Plc is contained within an SEM, so that the area hit by the laser beam can be accurately known and imaged.

2.4.2.1 Methods

Al stubs were cleaned thoroughly with ethanol. A cotton wool bud was used to sprinkle the volcanic ash onto the stub, which was then loaded into the SEM. The SEM was kept at low vacuum ~23 Pa. The fibres were probed first with the integrated EDS system, to check their chemical composition before the Raman analysis. NB. Samples must not have a c-coating on for Raman analysis. The carbon is a good Raman scatterer and this will interfere with the sample identification.
WD – 15 mm
EHT – 15 kV

2.4.2.2 Results

Sample Hawa_09 contained both blocky and fibrous $CaSO_4$. The blocky crystals, which were frequently observed, were identified as anhydrite ($CaSO_4$) by Raman-SEM, confirming the XRD spectrum for the bulk sample. The occasional fibrous crystals are confirmed to be gypsum ($CaSO_4.2H_2O$). The results are displayed in Figures 2.4.2 to 2.4.5 below.

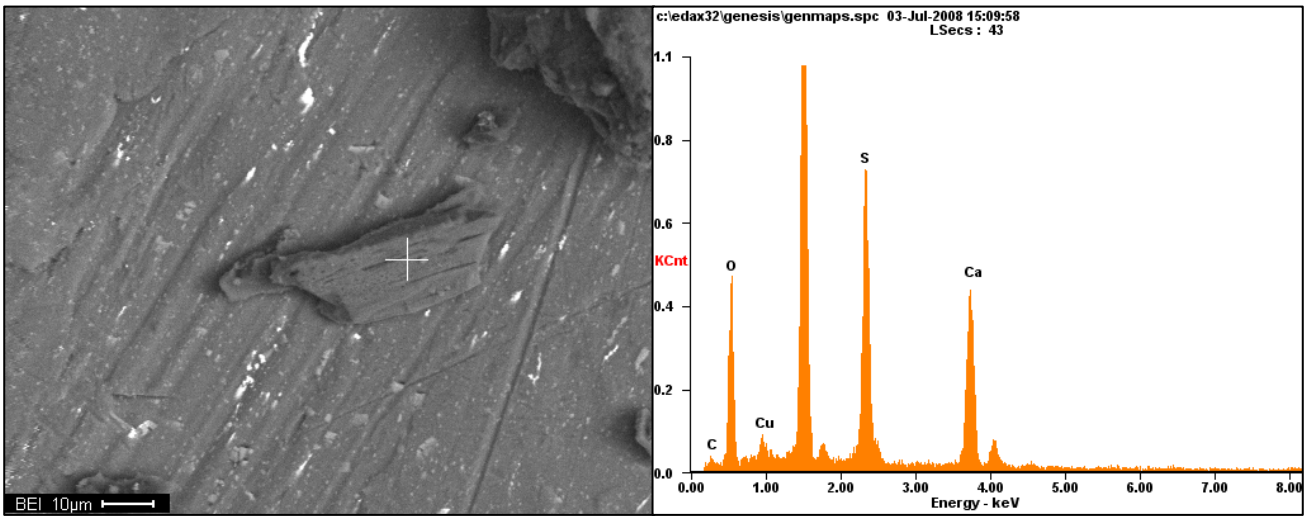

Figure 2.4.2 Blocky particle from the Hawa_09 sample and corresponding EDS spectrum.

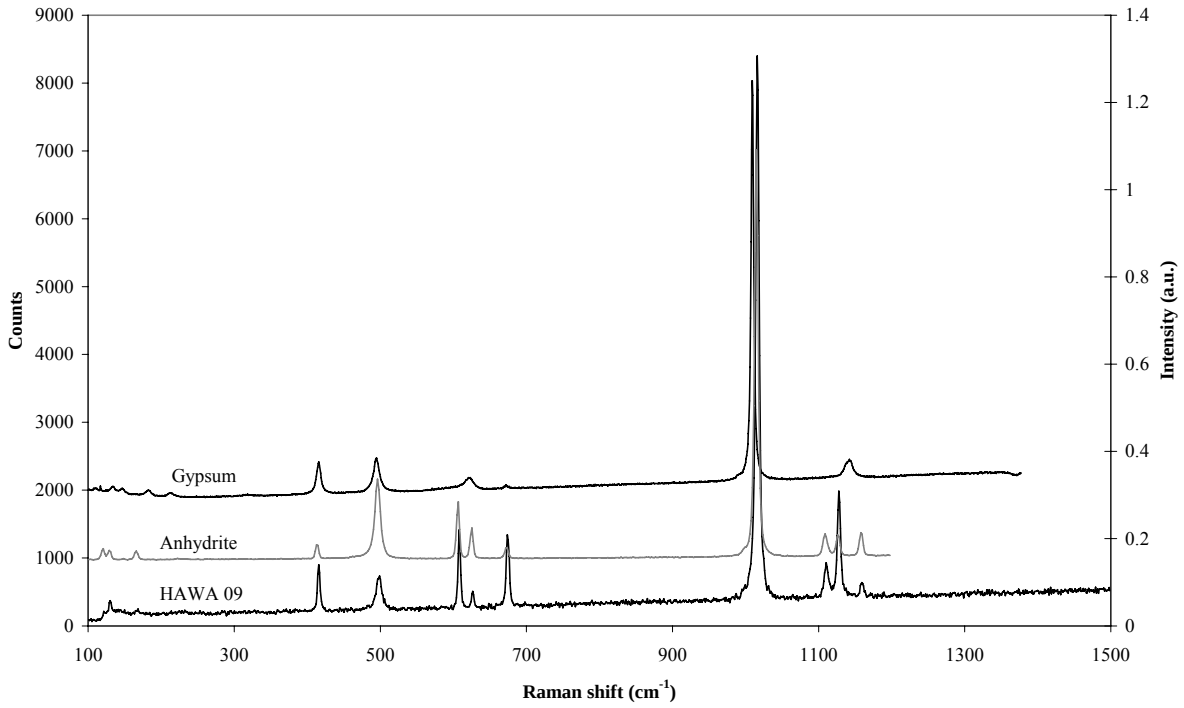

Figure 2.4.3 Raman spectrum from the particle shown in Fig 2.4.2 with library spectra for gypsum and anhydrite.

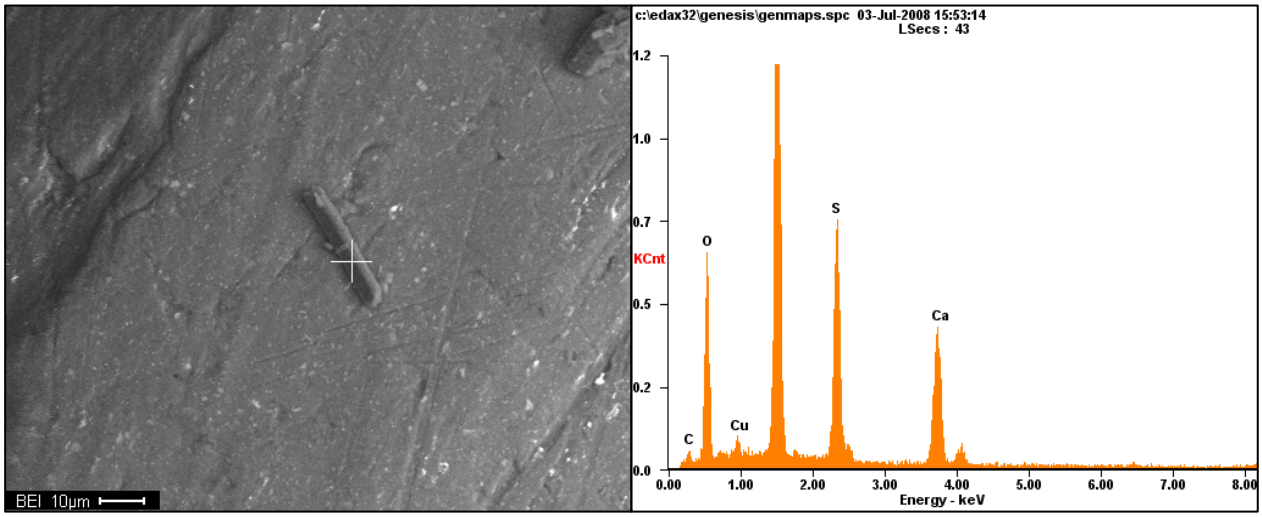

Figure 2.4.4 Fibrous particle from Hawa_09 sample and corresponding EDS spectrum.

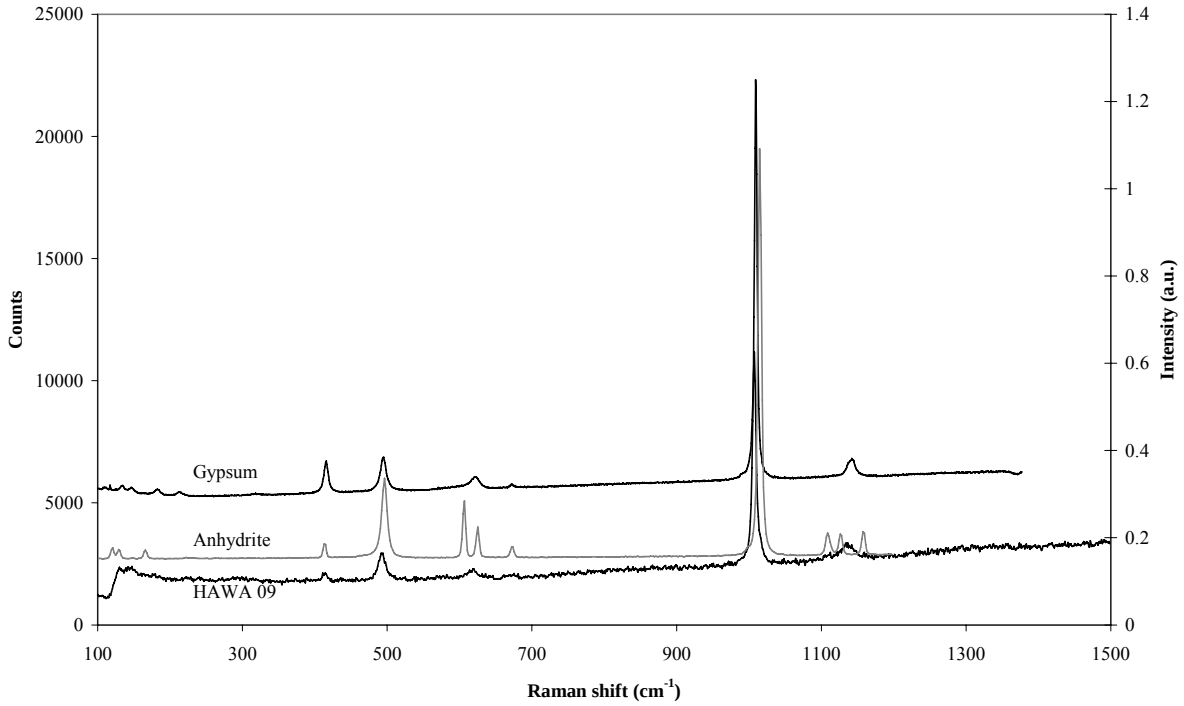

Figure 2.4.5 Raman spectrum from the particle shown in Fig 2.4.4

Library spectra from: Handbook of Minerals Raman Spectra
http://www.ens-lyon.fr/LST/Raman/index.php and published in
B. J. Berenblut, P. Dawson and G. R. Wilkinson, *Spectrochimica Acta Part A: Molecular Spectroscopy* **29**, 1973, 29-36[3]

2.5 Particle specific surface area – BET analysis

The specific surface area, combined with the surface reactivity, of a sample needs to be measured in order to determine the likelihood of particle toxicity within the lung. The calculation of 'surface area x surface reactivity' for any given sample, forms the basic model for cellular toxicity of insoluble compact particles (Prof. Ken Donaldson, pers. comm.) (see section 2.6 Particle Surface Reactivity). Particle surface area is also used for expressing dose in toxicological experiments, so knowledge of the surface area of the samples is useful if it is decided that toxicological tests are warranted at a later date.

Here we used the BET (Brunauer Emmet Teller) method of specific surface area analysis using nitrogen absorption with a Micromeritics TriStar 3000 Surface Area and Porosimetry Analyser in the Dept. of Chemistry, Durham University, for the Hawa_01 and Hawa_04 samples. The Hawa_09 sample was analysed using krypton absorption with a Micrometrics ASAP 2020 at the Università degli Studi di Torino, Italy. This was because the high levels of gypsum/anhydrite in this sample prevented the sample from adequately degassing for nitrogen absorption analysis. The nitrogen (Hawa_01 & 04) and the krypton (Hawa_09) data are not comparable.

2.5.1 Method

Prior to analysis, samples were degassed at 150 ºC for two hours.

2.5.2 Results

The specific surface area measured ranges from 0.15-3.9 m^2 g^{-1}.

Table 2.5.1. Results of the BET analysis to determine the surface area.

Sample	Specific surface area (m^2 g^{-1})	Error (+/- m^2 g^{-1})
Hawa_01*	0.8267	0.0032
Hawa_04*	0.1462	0.0007
Hawa_09§	3.9	

*Result is average of three runs using N_2. §Result is a single run using Kr.

Table 2.5.2 (below) allows comparison between the Hawaii samples and published data on specific surface area from volcanoes around the world. It can be seen that the Hawaii samples have specific surface areas in keeping with other ash samples except for the Hawa_09 sample which cannot be compared with previous nitrogen-analysed data.

Table 2.5.2. Surface area of various samples of volcanic ash (from Horwell et al., 2007[4]). Surface areas were measured by the BET (Brunauer Emmet Teller) method of nitrogen adsorption (Micromeritics Gemini Analyser with Flow Prep 060).

Volcano	**Surface area (m^2g^{-1})**
Cerro Negro, Nicaragua	0.47
El Reventador, Ecuador	1.53
Etna, Italy	0.19
Fuego, Guatemala	0.54
Langila, Papua New Guinea	0.9
Merapi, Indonesia	1.83
Mt St Helens, USA	1.62
Pacaya, Guatemala	0.21
Pintatubo, Philipines	0.89
Sakurajima, Japan	0.97
Soufrière Hills, Montserrat 1	1.28
Soufrière Hills, Montserrat 2	1.34
Tungurahua, Ecuador	0.72

.

2.6 Particle surface reactivity – EPR analysis

The surface reactivity of particles is often assessed by their ability to generate free or surface radicals. Recent work on volcanic ash has focussed on iron-catalysed free radical generation which is known to be potentially both a lung inflammation factor and a carcinogenic factor[5, 6]. Radical generation can become prolonged where the iron is present in a specific oxidative and coordinative state on the surface of the particulate matter[5-10]. Although iron is usually present in the Fe^{3+} oxidative state in crustal dusts, Horwell et al. (2003[11]) found that volcanic ash contains abundant Fe^{2+}. In the presence of hydrogen peroxide (produced naturally in the lungs), Fe^{2+} can catalyze the generation of hydroxyl radicals, through the Fenton reaction. Horwell et al. (2003[11]) found that andesitic volcanic ash generated abundant hydroxyl radicals (the Soufriere Hills, Montserrat ash) and Horwell et al. (2007[4]) showed that all ash types seem capable of generating hydroxyl radicals, but particularly basaltic ash (which is iron rich) which had previously been disregarded as a respiratory health hazard due to the lack of crystalline silica in these magma compositions.

Electron Paramagnetic Resonance (EPR) spectroscopy is employed for the identification of radicals on the surface of the volcanic ash. The amount of free radicals generated and released into solution can be quantified by using the spin-trapping technique[4, 11-14]. Since samples exhibit differences in surface area, results are expressed on a per unit surface area basis (see Section 2.5) to measure the real reactivity of the surface. A Miniscope 100 ESR spectrometer, Mag-nettech at the Università degli Studi di Torino, Italy was used in these experiments.

2.6.1 Method

EPR Spin-trap
The method replicates the Fenton reaction which may occur in the lung. 150 mg of the ash sample is suspended in 500 µL 0.5 M phosphate buffered solution at pH 7.4 (the pH of lung fluids), then 250 µL of 0.15 DMPO (the spin trap; 5,5'-dimethyl-1-pyrroline-*N*-oxide) and 500 µL H_2O_2 (0.2 mL 30 wt. % H_2O_2 in 10 mL H_2O) are added and the suspension stirred for 1 hour. During the 1 hour experiments aliquots of the suspension are withdrawn from a darkened vial after 10, 30 and 60 mins. and filtered through 0.25 µm filters. The liquid is introduced into a 50 µL capillary tube and placed in the EPR spectrometer. Each sample was tested at least twice and an average taken.

Receiver gain 9×10^2
Microwave power 10 mW
Modulation amplitude 1 G
Scan time 80 sec
Scans 2

The integrated amplitude of the peaks generated is proportional to the amount of radicals generated. The number of radicals is calculated by including a solid solution of Mn^{2+} in $CaCO_3$ as a calibration standard.

Iron release

Experiments were also carried out to characterise the amount of removable Fe^{2+} and Fe^{3+} from the surface of the ash as this represents the iron available for participation in the Fenton reaction (Fe^{3+} can be reduced to Fe^{2+} in the lung via the Haber Weiss cycle). Removable Fe^{2+} was measured through the use of ferrozine, a bidentate N donor chelator (pH 4) specific for Fe^{2+}, in the presence or in the absence of ascorbic acid, following a method previously described[4, 5, 11]. Since ascorbic acid reduces Fe^{3+} to Fe^{2+} the amount of iron measured in the presence of ascorbic acid corresponds to the total iron mobilised.

Samples (each of 20 mg) were placed in tubes with 20 mL of 1 mM solutions of ferrozine or ferrozine and ascorbic acid (1 mM). The suspensions were stirred at 37 °C. After 1 d the samples were removed and centrifuged for 15 min and an aliquot of the supernatant was analysed in a Uvikon spectrophotometer (at 562 nm) as ferrozine forms a coloured complex with Fe^{2+}. The samples were then returned to the incubator and measured in this way every 24 h for 9 days. A control solution of ferrozine with water showed no colour change over the experiment. As with the EPR data, the results are expressed per unit surface area.

2.6.2 Results

Figure 2.6.1 shows the hydroxyl radical generation results over the 60 minutes of each experiment. All samples generated the hydroxyl radical over the duration of the experiment. There is no consistent relationship in the kinetics of the experiment over time among the samples, however.

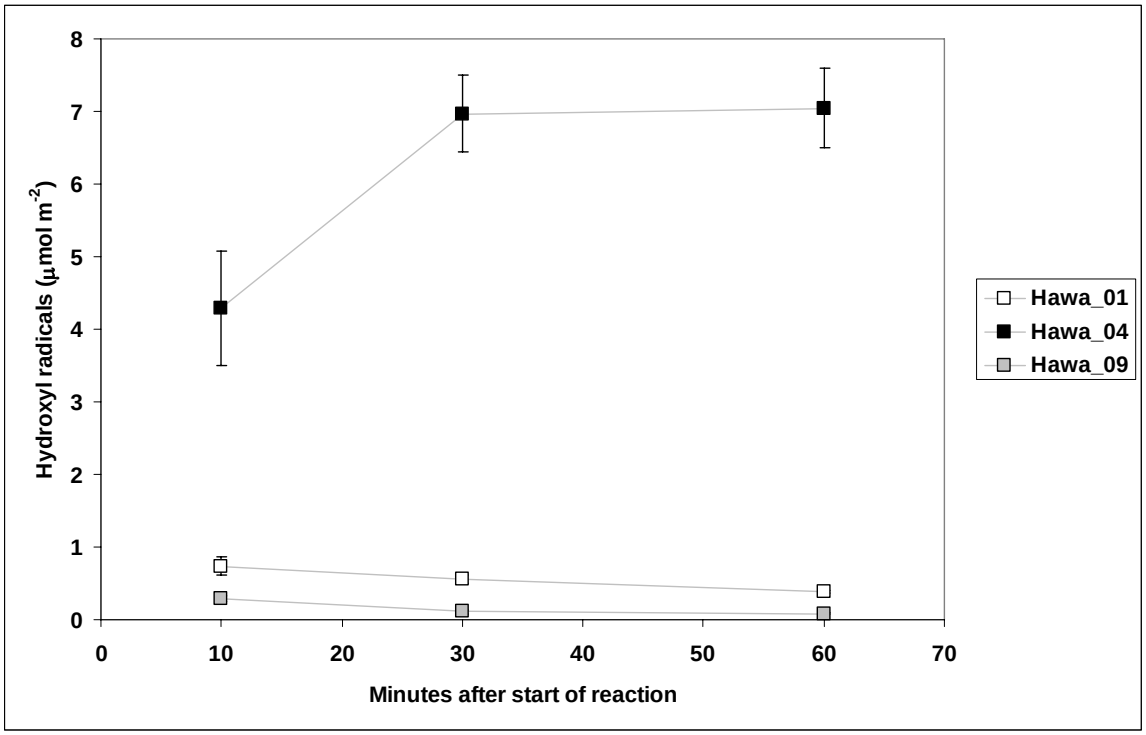

Figure 2.6.1 Production of hydroxyl radicals (per unit surface area) for the samples over the 60-minute experiments. Each value is the average of two experiments with error bars representing the standard error.

Figure 2.6.2 shows the results of the iron release experiments. As expected from the magmatic composition of the samples (Fig. 2.2.1), all of the samples displayed high iron release with Hawa_04 having much more total iron per unit surface area (728.2 µg m^{-2} after 7 days incubation) than the other two samples. These results are in keeping with basaltic samples from previously published work (e.g. total iron release after 7 days: Mt Etna 655.1 µg m^{-2}; Cerro Negro 389.2 µg m^{-2}; Pacaya 645.4 µg m^{-2})[4]. In terms of Fe^{2+}, the samples released less iron after 7 days than previously published data (e.g. Mt Etna 258.2 µg m^{-2}; Cerro Negro 177.4 µg m^{-2}; Pacaya 303.2 µg m^{-2}).

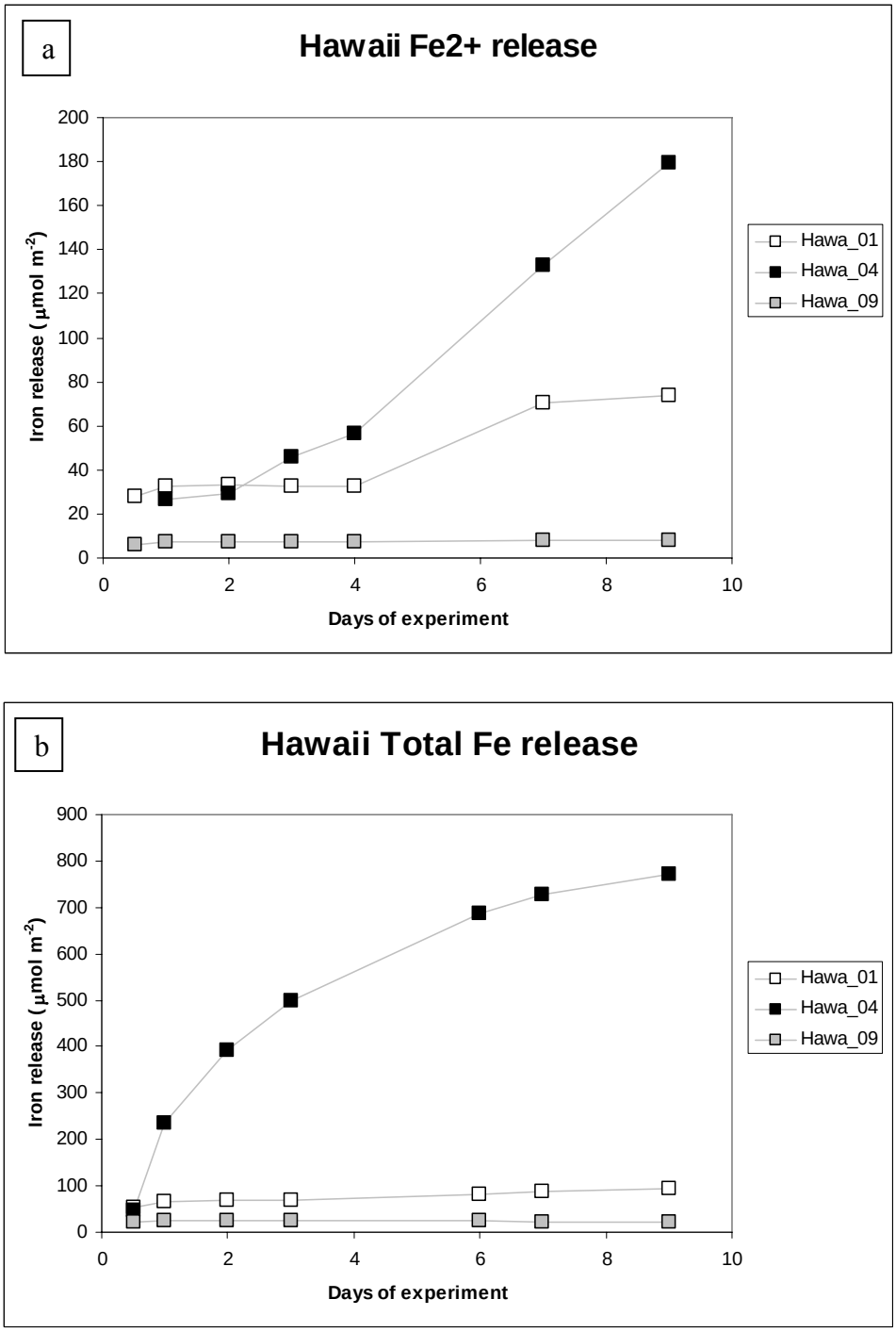

Figure 2.6.2. Amount of iron removed as a) Fe^{2+} and b) total iron during 9 days of incubation with chelators. The iron removed is expressed as amount per unit surface area.

The correlation between the amount of hydroxyl radicals generated after 30 min of incubation and the amount of iron released (in both oxidative states) after 7 d of incubation is reported in Figure 2.6.3.

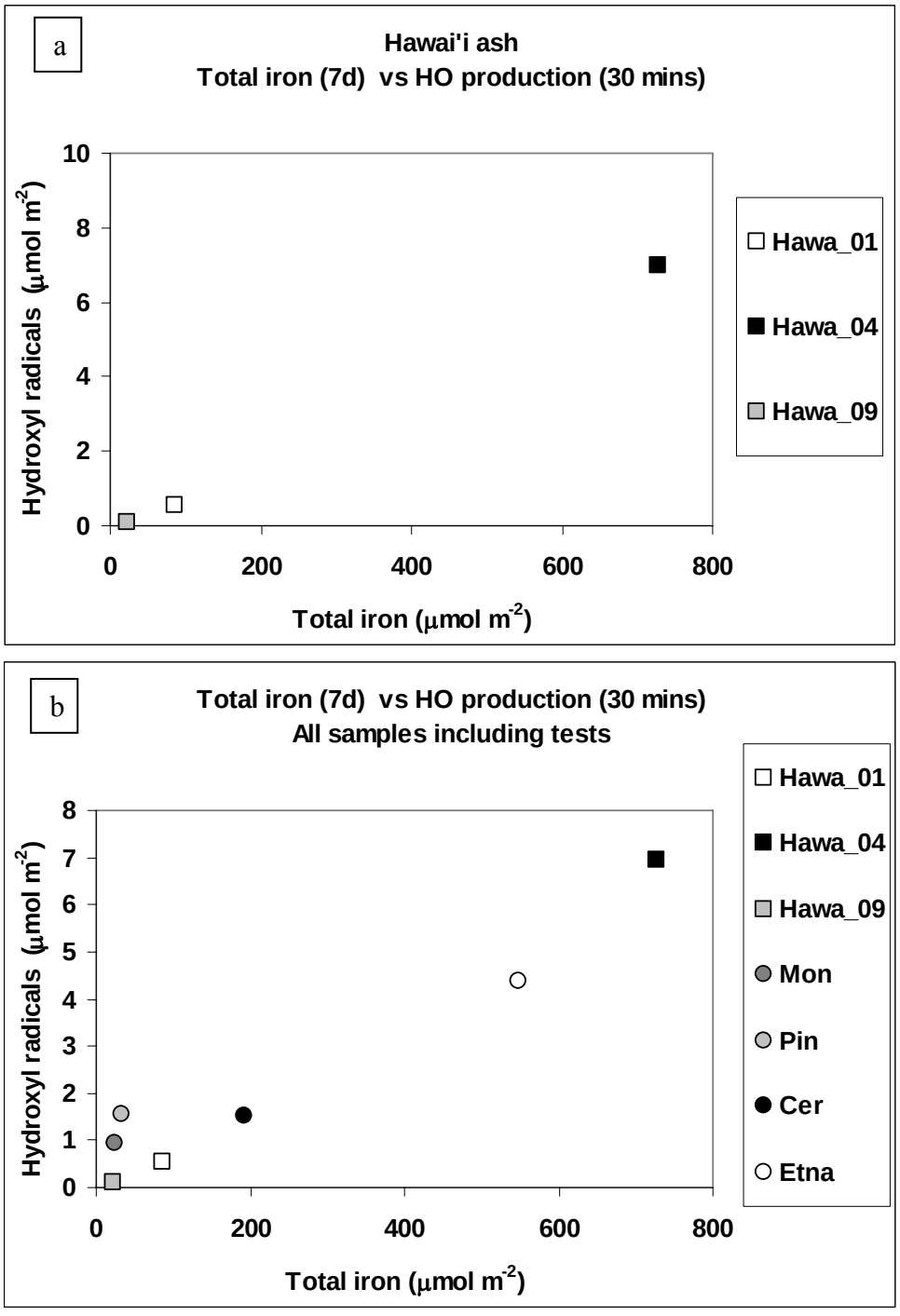

Figure 2.6.3 Amount of hydroxyl radicals generated after 30 min from the start of incubation versus total amount of iron extracted by chelators after 7 d. a) Hawai'i samples; b) Hawai'i samples and four samples previously used by Horwell et al. (2007). Mon = Soufrière Hills, Montserrat (5/6/99); Pin = Pinatubo (1991); Cer = Cerro Negro (1995); Etna = Mt. Etna, Sicily (2002) but analysed again for this work.

Figure 2.6.3 a) shows that, for the Hawai'i samples, there is a positive correlation between the amount of available iron for reaction and the number of radicals generated. To compare with previously published results, Figure 2.6.3 b) compares the Hawai'i samples with four ash samples of varying magmatic composition (basaltic to andesitic/dacitic) which were previously analysed by Horwell et al. (2007[4]). Here, these samples were re-analysed to check that the

current results were comparable with previously published results. The new and old data compared well. Figure 2.6.3 b) shows that Hawa_04 is capable of generating more radicals, and has more available iron, than any of the previously-analysed samples, including the basaltic Etna and Cerro Negro samples. The new data appear to form a linear trend with the other basaltic samples but it must be remembered that the results are displayed per unit surface area and we can not be sure that the surface area for Hawa_09 is similar to data that would have been obtained using nitrogen absorption.

3. Discussion and Conclusions

3.1 Particle size

The samples analysed for this report ranged from being extremely coarse grained, and typical of basaltic eruptions, to being more fine-grained than expected. The fine-grained nature of some of the samples is a likely result of the explosivity of the associated eruptions (e.g. Hawa_09 and associated explosion of 16 April 2008). The results here show that the potential health hazard of ash from Kilauea volcano differs depending on the eruption style and hazard managers should be aware that explosive eruptions are likely to generate significant quantities of respirable material.

When assessing the potential health hazard of the ash, as well as grain size, the duration and quantity of exposure are also vital parameters and should be taken into account in any health assessment.

3.2 Particle composition

Hawa_09 contained blocky and fibrous Ca-S in the form of anhydrite and gypsum. These minerals may have formed in several ways, for example: 1) Explosions may have erupted through near-surface fumaroles rich in hydrothermal minerals. 2) The lava may have interacted with deep hydrothermally-altered lavas. Bargar et al. (1995)[15] identified anhydrite blocks and gypsum fibres in cores extracted along the Kilauea Eastern Rift Zone. The minerals formed along with other hydrothermal minerals in open-space fillings in submarine lavas (>1500 m depth). Kullman et al (1994)[16] also identified gypsum fibres in airborne 'LAZE' samples at Kilauea, formed during interaction of lava with sea water at ocean entry points. Both gypsum and anhydrite are soluble minerals and are, therefore, not viewed as being a health hazard, even in fibrous form. A review of the carcinogenicity studies of fibrous gypsum in the Chemical Information Review Document issued for the US Department of Heath and Human Services (2006)[17] stated that one study found that gypsum fibres were weakly tumorigenic but all other studies have shown rapid clearance and dissolution in the lung.

Bargar et al.[15] and Kullman et al.[16] both identify crystalline silica polymorphs as being present as hydrothermal minerals in Kilauea emissions. Crystalline silica is not normally associated with basaltic eruptions but is the prime mineral of health concern in volcanic eruptions. We therefore recommend that the presence and quantity of crystalline silica polymorphs is assessed by X-ray Diffraction in order to fully assess the respiratory health hazard.

3.3 Surface reactivity

The results of the surface reactivity and surface area experiments are in line with previously published results[4] for basaltic samples. The data reported here suggest that the volcanic ash might represent a respiratory hazard through interaction of iron with hydrogen peroxide in the lung, generating the hydroxyl radical.

3.4 Differences among samples

The samples analysed for this study varied enormously in their grain size, morphological and compositional characteristics. Defining an overall hazard to the samples is, therefore, difficult but it is possible to say that the more explosive samples generate the most respirable material. The surface reactivity of the samples is not easily predicted and it is not clear whether the gypsum/anhydrite affected the reactivity of the samples or the surface area. However we can say that in some circumstances, the Kilauea ash certainly generates abundant hydroxyl radicals. It should be noted though that the sample with high surface area (Hawa_09) generated low numbers of radicals (per unit surface area) whereas a sample with low surface area and relatively low quantities of respirable particles (Hawa_04) generated large quantities of radicals. For significant toxicity to be a likely scenario, high surface area and high surface reactivity are needed and this was not the case for these samples.

3.4 Future hazard

Future eruptions from Kilauea may continue as present (low ash emission) but may also switch to a more explosive eruption style or a situation of continuous ash venting. In this case we strongly recommend a quantitative assessment of crystalline silica content, which we can carry out at Durham University.

3.5 Health message

The finer samples of Kilauea ash are sufficiently fine-grained to have the potential to trigger asthma attacks in susceptible people, and aggravate respiratory symptoms in people with chronic lung problems, if exposure is substantial. All people should wear masks in situations where exposure to the ash is going to be high, e.g., dry, windy days and where heavy traffic or tasks such as ash removal create dust in the air.

In public health terms, the potential for the development of long-term respiratory problems depends mainly upon the amount of crystalline silica in the ash and proportion of the ash which can be easily breathed into the deep parts of the lung. Taking the results of this study, and the experience acquired from other volcanoes over the last 25 years, the health hazard is low unless frequent eruptive activity commences which repeatedly exposes the population to high ash levels over long durations. In this case, careful monitoring of exposure and ash composition is required to make a full risk assessment.

3.6 Conclusions and suggested further work

The results of this study have found that the volcanic products from Kilauea volcano are basaltic, and can contain fine-grained, respirable particles.

The finer samples all generated hydroxyl radicals, with certain samples generating substantial quantities. We suggest that further analyses are carried out should ash emissions increase.

4. Further Information

The International Volcanic Health Hazard Network (IVHHN) is the umbrella organisation for people interested in the health effects of volcanic emissions.

Please refer to the IVHHN pamphlet on the health hazards of volcanic ash in order to learn more on the potential respiratory hazard posed by the Hawai'i ash.

Please also see the IVHHN Guidelines on Recommended Dust Masks.

All information can be found and downloaded from www.ivhhn.org including a copy of this report.

5. Acknowledgments

This work was funded through a UK Natural Environment Research Council (NERC) Urgency Grant NE/G001561/1.

The authors of the report wish to thank the following contributors:

Dr Peter Baxter, Institute of Public Health, University of Cambridge, UK
for providing the health assessment and message.

Mr Chris Rolfe, Geography Department, University of Cambridge, UK
for carrying out rapid grain size analyses.

Mr Nick Marsh, Department of Geology, University of Leicester, UK
for the XRF analysis.

Prof. Bice Fubini, Dr Maura Tomatis, Dr Ivana Fenoglio and Dr Francesco Turci, Università degli Studi di Torino, Italy
for guidance and help carrying out the surface reactivity analyses.

Prof. Ken Donaldson, MRC Centre for Inflammation Research at the University of Edinburgh,
for advice on particulate toxicity.

Dr Neil Cameron and PhD students, Durham University, UK
for help and advice during BET analysis.

Dr Alan Brooker, Renishaw Plc
for kindly allowing us to use the Raman-SEM facility without charge and for assistance with the analyses and interpretation.

6. References

1. Le Bas, M.J. & Streckeisen, A.L. The IUGS systematics of igneous rocks. *J. Geol. Soc. Lond.* **148**, 825-833 (1991).
2. Horwell, C.J. Grain size analysis of volcanic ash for the rapid assessment of respiratory health hazard. *J. Environ. Monitor.* **9**, 1107 - 1115 (2007).
3. Berenblut, B.J., Dawson, P. & Wilkinson, G.R. A comparison of the Raman spectra of anhydrite (CaSO 4) and gypsum (CaSO 4. 2H 2 O). *Spectrochim. Acta. A.* **29**, 29-36 (1973).
4. Horwell, C.J., Fenoglio, I. & Fubini, B. Iron-induced hydroxyl radical generation from basaltic volcanic ash. *Earth Plan. Sci. Lett.* **261**, 662-669 (2007).
5. Hardy, J.A. & Aust, A.E. Iron in asbestos chemistry and carcinogenicity. *Chem Rev* **95**, 97-118 (1995).
6. Kane, A.B. Mechanisms of Mineral Fibre Carcinogenesis. in *Mechanisms of Fibre Carcinogenesis* (ed. A.B. Kane, P. Boffetta, R. Saracci & J.D. Wilburn) 11-34 (International Agency for Research on Cancer, Lyon, 1996).
7. Smith, K.R. & Aust, A.E. Mobilization of iron from urban particulates leads to generation of reactive oxygen species in vitro and induction of ferritin synthesis in human lung epithelial cells. *Chem Res Toxicol* **10**, 828-834 (1997).
8. Ghio, A.J., *et al.* Role of surface complexed iron in oxidant generation and lung inflammation induced by silicates. *American Journal of Physiology* **263**, 511-517 (1992).
9. Fubini, B. & Otero Arean, C. Chemical aspects of the toxicity of inhaled mineral dusts. *Chem Soc Rev* **28**, 373-381 (1999).
10. Fubini, B. & Hubbard, A. Reactive Oxygen Species (ROS) and Reactive Nitrogen Species (RNS) generation by silica in inflammation and fibrosis. *Free Rad. Biol. Med.* **34**, 1507-1516 (2003).
11. Horwell, C.J., Fenoglio, I., Ragnarsdottir, K.V., Sparks, R.S.J. & Fubini, B. Surface reactivity of volcanic ash from the eruption of Soufrière Hills volcano, Montserrat, with implications for health hazards. *Environmental Research* **93**, 202-215 (2003).
12. Shi, X., *et al.* Generation of reactive oxygen species by quartz particles and its implication for cellular damage. *Applied Occupational and Environmental Hygiene* **10**, 1138-1144 (1995).
13. Fubini, B., Mollo, L. & Giamello, E. Free radical generation at the solid/liquid interface in iron containing minerals. *Free Rad Res* **23**, 593-614 (1995).
14. Fubini, B., Fenoglio, I., Elias, Z. & Poirot, O. Variability of biological responses to silicas: effect of origin, crystallinity, and state of surface on generation of reactive oxygen species and morphological transformation of mammalian cells. *J Environ Pathol Tox* **20**, 95-108 (2001).
15. Bargar, K.E., Keith, T.E.C. & Trusdell, F.A. Fluid-inclusion evidence for past temperature fluctuations in the Kilauea East Rift Zone geothermal area, Hawaii. *Geothermics* **24**, 639-659 (1995).
16. Kullman, G.J., Jones, W.G., Cornwell, R.J. & Parker, J.E. Characterization of air contaminants formed by the interaction of lava and sea water. *Environmental Health Perspectives* **102**, 478-482 (1994).
17. Integrated Laboratory Systems Inc. NC. Chemical Information Review Document for Synthetic and naturally mined gypsum. 24 (National Toxicology Program, National Institute of Environmental Health Sciences, National Institute of Health, US Department of Heath and Human Services, NC, 2006).
18. Horwell, C.J., Braña, L.P., Sparks, R.S.J., Murphy, M.D. & Hards, V.L. A geochemical investigation of fragmentation and physical fractionation in pyroclastic flows from the Soufriere Hills volcano, Montserrat. *J Volcanol Geotherm Res* **109**, 247-262 (2001).